EPJ AP
Applied Physics
EPJ.org
your physics journal

Eur. Phys. J. Appl. Phys. **97**, 22 (2022) **DOI:** 10.1051/epjap/2022210252

The electrode model of corona plasma discharge theory for current–voltage characteristics case in air

Asep Yoyo Wardaya, Zaenul Muhlisin, Jatmiko Endro Suseno, Qidir Maulana Binu Soesanto, Muchamad Azam, Evi Setiawati, and Susilo Hadi

edp sciences

The title “The European Physical Journal” is a joint property of EDP Sciences, Società Italiana di Fisica (SIF) and Springer

Eur. Phys. J. Appl. Phys. **97**, 22 (2022)
© EDP Sciences, 2022
https://doi.org/10.1051/epjap/2022210252

Special issue on 'Materials for Energy Harvesting, Conversion, Storage, Environmental Engineering and Sustainability', edited by M. El Ganaoui, M. El Jouad, R. Bennacer and J.M. Nunzi

THE EUROPEAN PHYSICAL JOURNAL APPLIED PHYSICS

Regular Article

The electrode model of corona plasma discharge theory for current–voltage characteristics case in air

Asep Yoyo Wardaya*, Zaenul Muhlisin, Jatmiko Endro Suseno, Qidir Maulana Binu Soesanto, Muchamad Azam, Evi Setiawati, and Susilo Hadi

Department of Physics, Faculty of Science and Mathematics, Diponegoro University, Semarang, Indonesia

Received: 7 November 2021 / Received in final form: 6 February 2022 / Accepted: 22 February 2022

Abstract. The calculation of the electrode model in the corona plasma discharge case has been carried out using the semi-ellipse line to plane (S-ELTP) configuration model in the air. The final focus of this research is to calculate the (I–V) current–voltage characteristics of the plasmas discharge. Part of the work in the (I–V) characteristics includes computational calculations and carrying out experimental activities. Experimental data include current vs voltage variations that occur at the time of plasma discharge. All the discharge processes are generated by a positive DC voltage source. The arrangement of the geometric configuration of the electrodes consists of two plates in the form of a half ellipse (active electrode) and a rectangular plate (passive electrode) in a mutually perpendicular position. The size variation of the active electrode includes variations of the small and large size plates with each plate having two variations in the distance between the two electrodes. The calculation concept of the electrode model is to insert the certain shape sharpness factor of k in the numerical calculation in the sharp electrode capacitance part. The k factor value is obtained by calculating the fitting between numerical simulation and research data. The research results prove that there is a fairly high level of conformity between numerical simulation and the research data. Simulation calculation for the (I–V) characteristic curve and its level of accuracy used Python GUI Programming.

1 Introduction

In 1928, Langmuir and Tonks gave the name plasma for the gaseous form ionized in an electric discharge [1]. At that time, many electronic devices use the concept of corona plasma discharge known as Capacitively Coupled Plasma (CCP) [2,3]. The name CCP was used because the working principle of this plasma device is similar to a capacitor even though it's different. The difference lies in the shape of the top electrode which is sharp at its endplate and always in the vertical position, while the other electrode is underneath and always in the horizontal position [4]. The role of CCP equipment is very important in research, especially in the formulation of corona currents that are in accordance with the physical phenomena that occur and as a function of voltage. Some of these research involve physical themes such as: the fluid model [5], electrohydrodynamic [6,7], Corona threshold [8], electric wind [9], mobility of large positive ions [10], and the empirical formula for negative corona discharge current [11].

In this study, we calculated the (I–V) characteristics of the CCP equipment with the configuration model of the semi-ellipse line to plane (S-ELTP) in the air. The calculation method does not use the concept of physical phenomena, but uses the physical visual concept of the corona current flow that came out of the sharp active electrode surface as done by [12–14]. The model electrode (S-ELTP) consists of two perpendiculars to each other plates, with a semi-ellipse shaped top plate is very sharp and facing downwards, while the bottom electrode is in the rectangular plate form which has a large enough surface area. In between, these two electrodes are given a DC voltage difference causing corona plasma discharge and the plasma electric current formed.

The CCP equipment is widely used in industry and to support various other researches such as ultra large-scale integrated circuit (ULSI) fabrication [15], modification of polymer materials surfaces [16], radio frequency plasmas [3,17], a lens-shaped electrodes [18], AC dielectric barrier discharges (DBD) [19] and etc. Likewise, various CCP models have been discussed in many papers such as point-to-plane [20,21], point-to-grid [11], point-to-cylinder [22], sphere-to-plane [23], coaxial cylinders [5], point-to-ring [10,24], etc. The use of the CCP is quite effective, because it can be generated with an ordinary DC current generator and can be made with simple technology but produces a large enough corona current output when compared to the current output of an ordinary capacitor system.

* e-mail: asepyoyowardayafisika@gmail.com

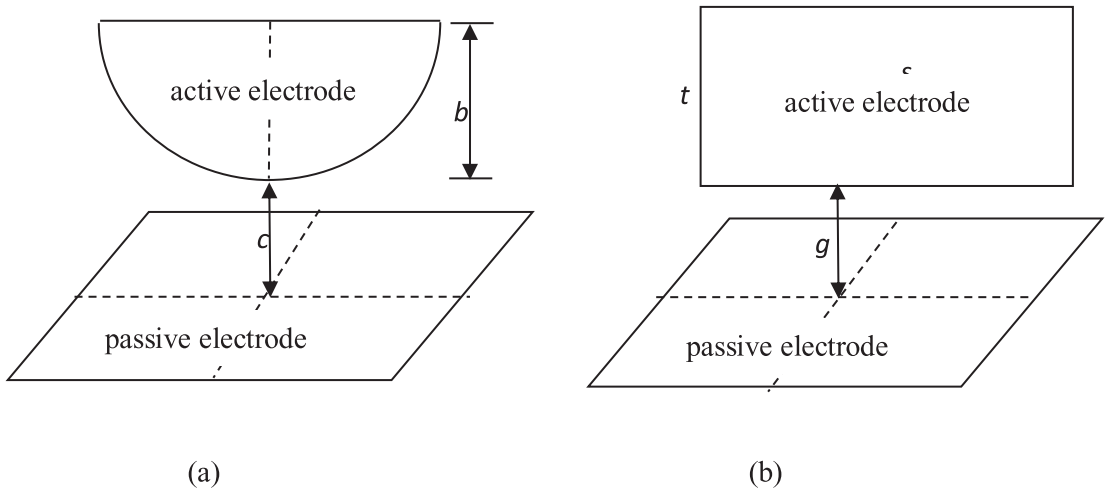

Fig. 1. Illustrated from the *S-ELTP* electrode configuration model (a) and the line-plane electrode configuration model (b). Both models have the same shape of the passive electrode, which is a rectangle lying under the active electrode. The active electrode in model (a) have the distances of the semi-major axis and semi-minor axis as a and b respectively and the distance between the two electrodes as c, while for model (b) each has length, width, and distance between the two electrodes as s, t, and g respectively.

The research scheme in this article is to calculate the electric current formulation as a voltage function of the S-ELTP configuration model. The formulation was used to validate the characteristics of the (I–V) current–voltage obtained from experimental data. There are several properties of plasma discharge in this CCP case that distinguish it from the working principle of capacitors in ordinary electronic circuits, namely:

– the emergence of a large enough plasma flow originating from the sharp surface of the active electrode (upper part) to the passive electrode (bottom part), which is due to the sharp geometrical surface properties that will have a high gradient potential (on the tip of the lower surface of the active electrode) [4].
– from the research [25], it was concluded that the smaller the sharpness angle of the electrode tip will result in an increase in the size of the resulting plasma, which applies to all types of the same electrodes material but has different sharpness angle variations at the tip of the electrode.

As for the concept of the research that we carried out, one of the factors was caused by the nature of the plasma discharge in the CCP case which showed a tendency for plasma flow to become larger and stronger when it came out of the tip of the electrode, which became sharper in the shape (electrode geometry). From the research results of [25], it was found that the geometric effect of the sharp electrode shape greatly affects plasma flow in the case of coronal plasma discharge. This geometric effect is realized in this study through the calculation of the "modified capacitance model" as described in [12–14]. The calculation method of this model is the same as the usual capacitance calculation, but is modified by adding a multiplier factor (an electric current multiplier) of k to the sharpest part of the active electrode boundary condition. Through the relationship between the corona current and the formulation of the modified capacitance and the applied voltage, the current graph will increase quite high in the (I–V) characteristic case, because apart from being a function of voltage, it also depends on the k factor which is in the modified capacitance formulation. The value of k is not obtained through a formula calculation but through a fitting value that matched between the numerical calculations results and the experimental data on the (I–V) characteristic curve of the corona discharge.

2 Mathematical models

The formulation form of the (I–V) characteristic model has been widely expressed in various studies such as by [7–11] through the following equation

$$I = C_1 V(VV_i) \tag{1}$$

where C_1 is a constant and V_i is the initial corona discharge voltage. According to [9], the constant C_1 is a function of geometry. There is another (I–V) model, as revealed by [6,12–14,26], through the following equation:

$$I = C_1(V)^2, \text{ with } (V) = VV_i. \tag{2}$$

Our research is based on the choice of equation (2), where the constant C_1 in equation (2) is a function of the capacitance model undergoing renewal (with the addition of the k-shape sharpness factor) [12–14] from the electrode configuration model in the corona plasma discharge. The shape of the active electrode is a semi-ellipse with the curved part facing downwards. The electrode has a size of half the long axis of a and half of the short axis of b and a thickness of $\delta \cong 0.0001$ m. While the passive electrode (rectangular shape) is in a horizontal lying position at a distance of c below the active electrode. The illustration of the *S-ELTP* electrode configuration can be seen in Figure 1a. To produce a

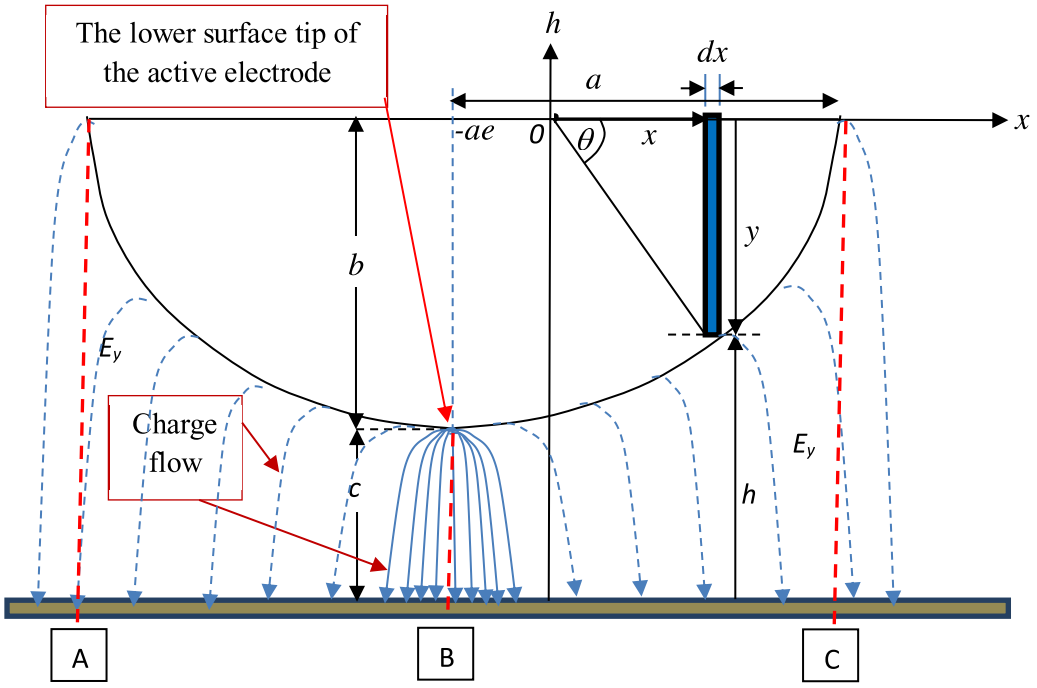

Fig. 2. The approach of the *S-ELTP* electrode configuration consists of two thin electrodes with the position of the active electrode perpendicular to the passive electrode and the distance between the two electrodes is c. Points A, B, and C are the left, middle, and right end boundary points respectively on the x-axis of the active electrode.

corona plasma discharge, which subsequently produces an electric current, we put a DC voltage difference of V between two electrodes.

Before calculating the capacitance value from the *S-ELTP* electrode configuration, the reference capacitance value from the line-plane electrode configuration model is set. According to [12,14], if there is a rectangular electrode plate in an upright position (the active electrode) that has a length s and a width t and there is a rectangular electrode in a lying position (the passive electrode), where the distance between electrodes is g (illustrated in Fig. 1b), then the capacitance value can be written as

$$C = {}_0 s \ln |\frac{t}{g} + 1|. \tag{3}$$

The electrode configuration model of the semi-ellipse line to plane (S-ELTP) in the air is part of the CCP model composed of two perpendiculars each other plates, with a semi-ellipse shaped top plate is very sharp and facing downwards, while the bottom electrode is in the rectangular plate form which has a large enough surface area. In between, these two electrodes are given a DC voltage difference causing corona plasma discharge and the plasma electric current formed. The semi-elliptical shape of the S-ELTP active electrode model has a major half axis of a and a half minor axis of b, and the ratio between the distance from the center of the ellipse to the focus of the ellipse to the distance a is called the eccentricity quantity [27]. The form of plasma flow that is formed mostly comes out from the bottom center (the sharpest part) of the active electrode and the rest will come out along a curved path from the active electrode to the passive electrode. The shape of the plasma ion flow that flows from the active electrode to the passive electrode is not directed straight down, but has a curved contour following the shape of an elliptical curve with the greatest value of the electric field, of course, at the bottom and center of the active electrode.

To calculate the capacitance form of the S-ELTP configuration model, we refer to the capacitance values of the CCP model from the line to plane configuration model in equation (3) [12,14]. The model was chosen because it has a rectangular active electrode. If the area of the active electrode from the S-ELTP model is divided into rectangular area elements, each of which represents its capacitance elements, then by comparing the values of the plate area and capacitance in the line to plane model with the rectangular area elements plate and capacitance elements in the S-ELTP model (the model sketch in Fig. 2), it can be calculated the capacitance value which is the integral of the capacitance element of the S-ELTP configuration model. In Figure 2, we can see there is symmetry between the right and left sides of the ellipse coordinate center of (0,0). Due to the

symmetrical nature, the capacitance calculation in Figure 2 only includes part of the active electrode to the right of the coordinate center.

By using the concept of equation (3), which is applied to the element area of the rod in Figure 2, the magnitude of the capacitance element is obtained as follows:

$$dC = {}_0\, dx \ln|\frac{y}{h} + 1| = {}_0\, dx \ln|\frac{b+c}{h}|. \tag{4}$$

The definition of the variable h and the eccentricity number at the elliptical coordinates (e) in Figure 2 can be written as,

$$h = b + cy; e = \sqrt{1(b/a)^2}; b \le a. \tag{5}$$

The relationship between the x and y-axis as the function of θ in the elliptical coordinates which is illustrated in Figure 2 defined as

$$x = \frac{a(1e^2)\cos\theta}{1 + e\cos\theta}; y = \frac{a(1e^2)\sin\theta}{1 + e\cos\theta}. \tag{6}$$

The value of the derivative dx as a function of θ and the limits of integration of θ is written as

$$\mathrm{d}x = a\big(1e^2\big)\frac{\sin\theta\, d\theta}{(1 + e\cos\theta)^2}; \tan^1\frac{b}{ae} \le \theta \le 0. \tag{7}$$

By substituting equations (5)–(7) in equation (4), we obtain the value of the capacitance element as a function of θ:

$$dC = \frac{{}_0\, b^2\sin\theta}{a(1 + e\cos\theta)^2}\ln|1 + \frac{b^2\sin\theta}{a(b+c)(1 + e\cos\theta)}|\, d\theta. \tag{8}$$

Suppose we know a form of the following mathematical concept,

$$\int u\, d\, v = uv\int v\, d\, u \tag{9}$$

with

$$u = \ln|1 + \frac{b^2\sin\theta}{a(b+c)(1 + e\cos\theta)}|;\ v = (1 + e\cos\theta)^1. \tag{10}$$

The calculation models in equations (9)–(10) can be used to solve equation (8), where there is a relationship

$$C = \int dC = \frac{{}_0 b^2}{ae}\int u\, dv;\ dv = \frac{e\sin\theta}{(1 + e\cos\theta)^2}\, d\theta \tag{11}$$

where u and v are dimensionless variables. If the final solution of equation (8) can be solved with using the θ integration boundary in equation (7), by using the following definition in integral table [28] as,

See equation below.

where

$$A_0 = \frac{\begin{matrix} A & B & C \\ | a_1 & b_1 & c_1 | \\ a_2 & b_2 & c_2 \end{matrix}}{|\begin{matrix} a_1 & b_1 \\ a_2 & b_2 \end{matrix}|^2 |\begin{matrix} b_1 & c_1 \\ b_2 & c_2 \end{matrix}|^2 + |\begin{matrix} c_1 & a_1 \\ c_2 & a_2 \end{matrix}|^2},$$

$$A_1 = \frac{|\begin{matrix} |\begin{matrix} B & C \\ b_1 & c_1 \end{matrix}| & |\begin{matrix} A & C \\ a_1 & c_1 \end{matrix}| & |\begin{matrix} B & A \\ b_1 & a_1 \end{matrix}| \\ a_1 & b_1 & c_1 \\ a_2 & b_2 & c_2 \end{matrix}|}{|\begin{matrix} a_1 & b_1 \\ a_2 & b_2 \end{matrix}|^2 |\begin{matrix} b_1 & c_1 \\ b_2 & c_2 \end{matrix}|^2 + |\begin{matrix} c_1 & a_1 \\ c_2 & a_2 \end{matrix}|^2},$$

$$A_2 = \frac{|\begin{matrix} |\begin{matrix} C & B \\ c_2 & b_2 \end{matrix}| & |\begin{matrix} C & A \\ c_2 & a_2 \end{matrix}| & |\begin{matrix} A & B \\ a_2 & b_2 \end{matrix}| \\ a_1 & b_1 & c_1 \\ a_2 & b_2 & c_2 \end{matrix}|}{|\begin{matrix} a_1 & b_1 \\ a_2 & b_2 \end{matrix}|^2 |\begin{matrix} b_1 & c_1 \\ b_2 & c_2 \end{matrix}|^2 + |\begin{matrix} c_1 & a_1 \\ c_2 & a_2 \end{matrix}|^2},$$

$$\left[|\begin{matrix} a_1 & b_1 \\ a_2 & b_2 \end{matrix}|^2 + |\begin{matrix} c_1 & a_1 \\ c_2 & a_2 \end{matrix}|^2 \ne |\begin{matrix} b_1 & c_1 \\ b_2 & c_2 \end{matrix}|^2\right] \tag{12}$$

and

$$\int \frac{\mathrm{d}x}{(a + b\cos x + c\sin x)} = \frac{2}{\sqrt{a^2b^2c^2}}\tan^1\left\{\frac{(ab)\tan(\frac{x}{2}) + c}{\sqrt{a^2b^2c^2}}\right\}, \text{for}\left[a^2b^2 + c^2\right] \tag{13}$$

$$\int \frac{(A + B\cos x + C\sin x)\, dx}{(a_1 + b_1\cos x + c_1\sin x)(a_2 + b_2\cos x + c_2\sin x)} = A_0\ln|\frac{a_1 + b_1\cos x + c_1\sin x}{a_2 + b_2\cos x + c_2\sin x}| + A_1\int\frac{\mathrm{d}x}{(a_1 + b_1\cos x + c_1\sin x)} + A_2\int\frac{\mathrm{d}x}{(a_2 + b_2\cos x + c_2\sin x)}$$

then the modified capacitance value of equation (8) is obtained as

See equation (14) below.

in the case of $[a(b+c)]^2 > [a(b+c)\,e]^2 + b^4$. For the usual integration case, the value of the shape sharpness factor of k is 1 in equation (14). This factor is deliberately introduced at the boundary conditions for the integration of the sharpest surface at the lower end of the active electrode, namely at the boundary between points c and b in Figure 2, or at the coordinates of

$$(x, y) = (ae, b) \text{ or } \theta_1 = \tan^1 \frac{b}{ae}. \tag{15}$$

The emergence of the k factor is a manifestation of the geometric properties of the constant C_1 in equation (2). This geometrical property is demonstrated by a large enough plasma flow at the sharpest surface compared to other surfaces at the active electrode in the capacitance calculation [12,14]. The calculation of the value of k is based on the value of the match between the numerical calculations and the experimental results. One more thing, the solution to equation (14) is taken in the half-part condition of the active electrode (from the middle to the right end) in Figure 2 because of the symmetrical nature of the elliptical mathematical concept. To understand the concept of the geometric visual effect of the shape of the active electrode, We review again Figure 2, but only present the horizontal boundary conditions at points A, B, and C. In the figure, the sharpest part of the active electrode is in the middle of the bottom (in line with the boundary condition of a point B). The expression of the number k is a multiplier factor (current multiplier) in a sharp part of the active electrode region. The value of the k is entered in the boundary conditions for the integration of the capacitance manually in the area that is in line with point B, through the following equation,

$$C_{tot} = \int_A^C dC = 2\int_{kB}^C dC = 2C. \tag{16}$$

So, there is the k multiplier factor that appears in the boundary conditions of integration in point B for the case of the corona current.

To calculate the value of electric current flowing from the active electrode to the passive electrode, there are several assumptions as follows [12–14]:

– the magnitude of the electric charges and electric field flowing from the active electrode to the passive electrode is

$$q = C_{tot}(V).; E_y = \frac{q}{{}_0A} = \frac{C_{tot}(V)}{{}_0\{2\delta a + \delta^2\}} \tag{17}$$

where the notations A and δ are the Gaussian surface area and the thickness of the active electrode ($\delta \cong 0.0001$ m), respectively.

– equation of electric current using the concept of equation (2).

– the values of space permittivity and permeability in air replaced with space permittivity ${}_0$ and permeability μ_0 (in a vacuum) because the difference is not too significant,

$$C \cong \frac{{}_0 b^4}{ae}\left\{\begin{array}{l} \dfrac{1}{[a(b+c)(1+e)]}\dfrac{k\left(\dfrac{e(a+b)}{\sqrt{b^2+(ae)^2}}+\dfrac{a^2e^3}{b^2+(ae)^2}\right)}{\left[a(b+c)+\dfrac{a^2e^2(b+c)+b^3}{\sqrt{b^2+(ae)^2}}\right]}\dfrac{1}{\left(1+\dfrac{ae^2}{\sqrt{b^2+(ae)^2}}\right)} \\ +k\dfrac{2\sqrt{1e^2}}{b^2(1+e^2)}\tan^1\left[\dfrac{(1e)}{\sqrt{1e^2}}\dfrac{b}{\left(ae+\sqrt{b^2+(ae)^2}\right)}\right] \\ \dfrac{e}{b^2(1+e^2)}\left\{\ln|\dfrac{1}{a(b+c)}|k\ln|\dfrac{\sqrt{b^2+(ae)^2}+ae^2}{a(b+c)\sqrt{b^2+(ae)^2}+a^2(b+c)e^2+b^3}|\right\} \\ \left[\dfrac{2a(b+c)(e^21)+2b^2e^2}{b^2(1+e^2)\sqrt{[a(b+c)]^2[a(b+c)e]^2b^4}}\right]\otimes \\ \otimes\left\{\tan^1\left[\dfrac{b^2}{\sqrt{[a(b+c)]^2[a(b+c)e]^2b^4}}\right]k\tan^1\left[\dfrac{\dfrac{ba(b+c)(1e)}{ae+\sqrt{b^2+(ae)^2}}+b^2}{\sqrt{[a(b+c)]^2[a(b+c)e]^2b^4}}\right]\right\} \end{array}\right\}, \tag{14}$$

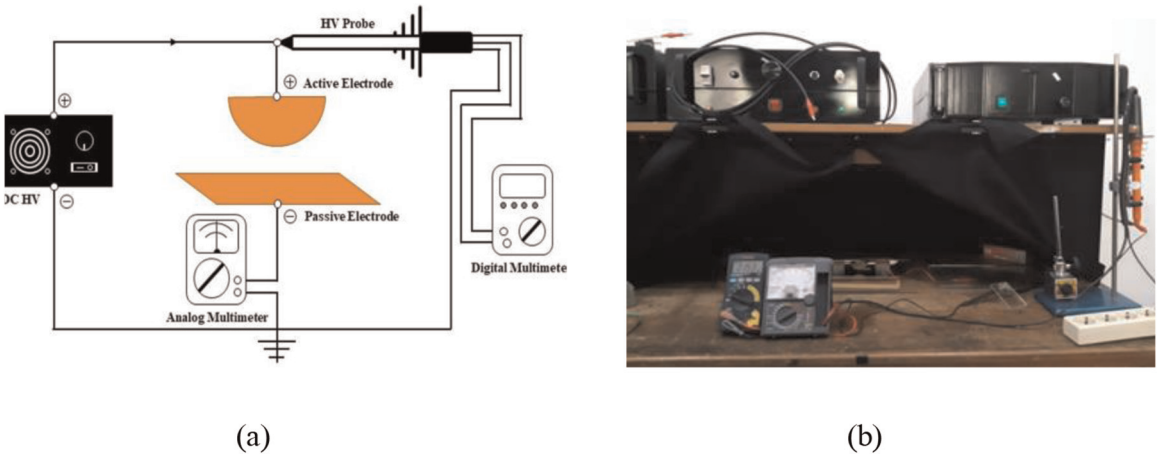

Fig. 3. (a) Circuit schematic and (b) photograph of the equipment circuit of the plasma discharge reactor from the *S-ELTP* electrode configuration model.

namely for conditions in the air at STP, 900 kHz are $=1.00058986\ _0$ and $\mu=1.00000037\ \mu_0$ with values $_0=8.854\times10^{-12}$ F m^{-1} and $\mu_0=4\times10^{-7}$ Hm^{-1}.

By using these three assumptions, the magnitude of the electric current as a function of the potential at the resulting *S-ELTP* electrode configuration is equal to:

$$I=\frac{dQ}{\mathrm{d}t}=\frac{\mu}{V}\left(qE_y{}^2\right)_{total}=\frac{\mu_0}{_0{}^2}|\frac{\{C_{tot}\}^3}{\left(2\delta a+\delta^2\right)^2}|(VV_i)^2. \quad (18)$$

Equation (18) relates between the values of the current I, total capacitance C_{tot}, and voltage V. In the C_{tot} contains the modified capacitance C, as written in equation (14). So it is clear that the corona current depends on the variation of the voltage change V and also depends on the plasma flow that came out of the sharp edge of the active electrode (with the emergence of the k factor). Equation (18) is used to simulate the (I–V) characteristics of the electrode model with the *S-ELTP* configuration. The simulation model uses *Python Graphical User Interface (GUI) Programming* which can present graphs while showing several parameters of the level of accuracy adjustment between the simulation graph and experimental data.

3 Experiment technique

The schematic of the plasma discharge reactor apparatus of the *S-ELTP* electrode configuration is based on the following working steps:

– electrodes with the *S-ELTP* configuration are connected to a high voltage DC generator (4 kV voltage and 25 kHz frequency).
– the main circuit is connected in series with an electric current measuring device (Ampere meter), namely SANWA analog multimeter (type YX-360TREB, voltage 220 V, and frequency 50/60 Hz).
– for measuring the potential differences, a SANWA digital multimeter (voltmeter) is used (type CD771).
– there is equipment that can convert kV units to Volts, namely the HV probe (Maximum Voltage 40 kV DC, model number: AC 28 kV PD-28, serial number: 01605733). In this case, the electric current passed through the HV probe before passing through the voltmeter.

In Figure 3, the circuit schematic and photos of the plasma discharge reactor equipment circuit are shown from the *S-ELTP* electrode configuration model.

4 Results

In this research, we present two size variations of the active electrode, which are named as small and large size electrodes, respectively. The passive electrode is presented as a rectangular plate that is large enough, so it can be used by both size variations of the active electrode. There are two variations of the value of c for each of these electrode sizes. All these experiments satisfy the capacitance value rules as shown in equation (11). The length of semi-major and semi-minor axes are a and b respectively, the distance between the two electrodes is c, and the eccentricity number on the elliptical coordinates is e that can be written for two-electrodes size case as,

– the small size electrode:
$a=0.025$ m; $b=0.024$ m

$$e=\sqrt{1(b/a)^2}=\sqrt{1(2.4/2.5)^2}=0.28$$

Variations of c values are 0.009 m and 0.033 m.

– the large size electrode:
$a=0.05$ m; $b=0.045$ m.

$$e=\sqrt{1(b/a)^2}=\sqrt{1(4.5/5)^2}=0.436$$

Variations of c values are 0.039 m and 0.042 m.

The research data taken in this study are variations of current and voltage data when the corona discharge process occurs. When the V_i initial voltage is applied in this experiment, electric current has not appeared. If the

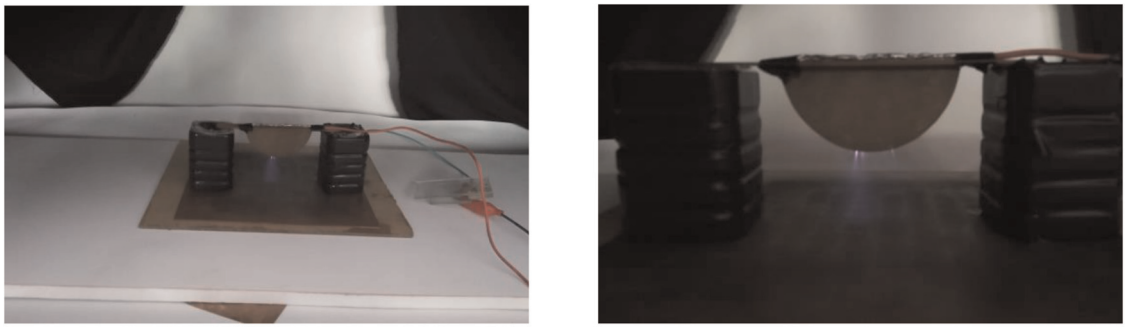

Fig. 4. The appearance of the largest plasma flow coming out of the lower end (in the middle position) from the active electrode to the passive electrode, in the two cases of the small (a) and large (b) size electrodes.

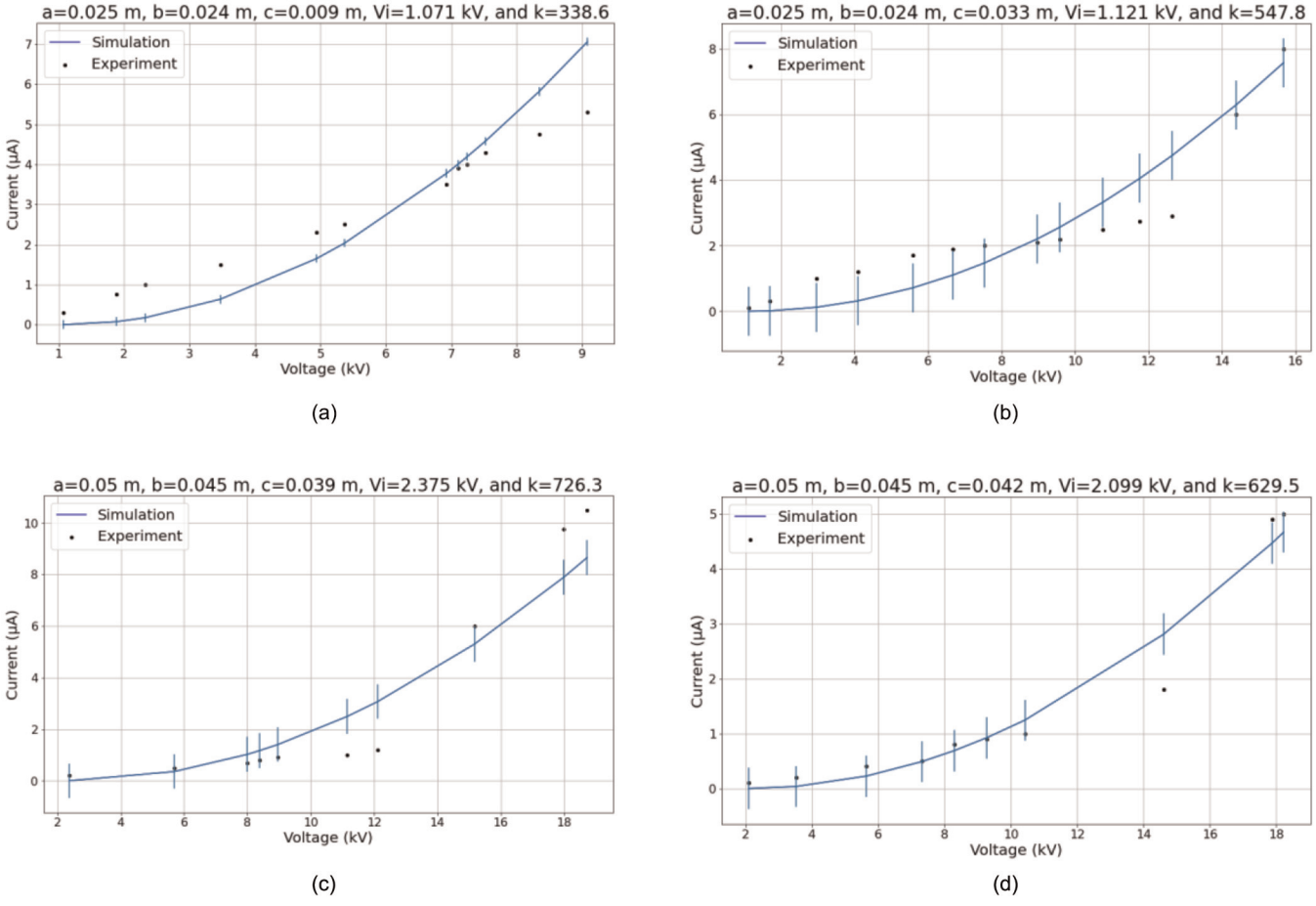

Fig. 5. The (I–V) characteristics graph of the electrode model with the *S-ELTP* configuration. For the small size electrode shown in (a) with $c = 0.009$ m; $k = 338.6$ and (b) with $c = 0.033$ m; $k = 547.8$. As for the large size electrode, it is shown in (c) with $c = 0.039$ m; $k = 726.3$ and (d) with $c = 0.042$ m; $k = 629.5$.

voltage variation is enlarged, it will begin to read the appearance of an electric current that is also getting bigger, known as the Townsend discharge [29]. When the voltage is increased again, it will read a significant increase in current known as the corona discharge. The photos of experimental results from corona plasma discharge with the *S-ELTP* electrode configuration are shown in Figure 4. In Figures 4a and 4b (for the case of the small and large size electrodes, respectively), we can see that the largest flow of corona plasma discharge comes from the very bottom (in the middle position) of the active electrode.

Table 1. List of the k factor and measurement parameters from the level of accuracy for the (I–V) characteristic graph from various sizes of electrodes in Figure 5.

Electrode Size	c (meter)	k	*t-test*	*SD*	Number of tangent points	Number of data points	Percentage of tangent points
Small	0.009	338.6	0.0412	0.1075	1	12	8.33%
Small	0.033	547.8	0.0495	0.7467	9	14	64.29%
Large	0.039	726.3	0.0495	0.6704	6	10	60.00%
Large	0.042	629.5	0.0461	0.3754	8	10	80.00%

The simulation and experimental results of the (I–V) characteristics of the electrode model with the *S-ELTP* configuration for the small and large size electrodes are presented in Figure 5. In the Figure, there are two variations of the value of c for the size of each electrode with the simulation calculation using equation (15). Besides displaying the fitting value of the appropriate k factor, the calculation of the parameters of the level of accuracy between the simulation results and experimental data is also displayed. These parameters include the values of the *t-test* and standard deviation (*SD*), which are shown in Table 1. The results of the characteristic graph calculations along with their accuracy levels, all of which are processed using *Python Graphical User Interface* (GUI) *Programming*.

The relationship between the k factor value and the measurement parameters of the accuracy level for the (I–V) characteristic graph can be explained as follows:

- the k value is determined by the sharpness of the electrode tip [12–14]. In general, the sharper the electrode tip, the greater the k value.
- the *t-test* value is a statistical parameter that relates the degree of correspondence between the numerical calculations (curve lines) and the research results (data points) [30] of the (I–V) characteristic graph. For a high level of accuracy, the *t*-test value should be lower than 0.05.
- the *SD* (standard deviation) value in this *Python GUI Programming* [31] takes the form of the 2nd order of the following polynomials

$$I = a_1 + a_2 V + a_3 V^2 \tag{19}$$

where a_1, a_2 and a_3 are countable constants. Equation (19) is compatible with the formulation models of equations (2) and (18) so that there is a match between the numerical simulation formula and the *SD* formulation.

There are several important notes obtained from Table 1, namely

- in the case of a small electrode size with a value of $c = 0.009$ m, it turned out to have the smallest k value compared to other cases.
- the *t*-test values all have values below 0.05, which indicates the high level of accuracy of this research, with the lowest *t-test* value, which shows the highest level of accuracy is also shown in the case of a small electrode size with a value of $c = 0.009$ m.
- similarly, the standard deviation (*SD*) value with the highest level of accuracy (lowest *SD* value) was obtained in the case of a small electrode size with a value of $c = 0.009$ m.
- in Figure 5, there are various short vertical lines (*svt*) connecting the data points with the simulation curve. If the length of the *svt* gets smaller then the higher the level of accuracy between the data points with the tangent of the simulation curve, which is indicated by the smaller *t-test* and *SD* values in Table 1.
- in the case of research that is not very perfect (in this study), then if the length of *svt* is small enough it will produce a large number of data points that are not connected to the simulation curve. For research case with $k = 338.6$ in Table 1, which has the smallest *t-test* and *SD* values, only has a number of tangent points (*ntp*) of three. The *ntp* is the number of data points connected to the simulation curve through the *svt*. The percentage of tangent points (*ptp*) is obtained which is the ratio between the ntp and the number of data points (ndp) whose value is only about 8.33%.
- in Table 1 for the other three cases besides $k = 338.6$, they have a fairly large *t-test* and SD value, so they have the *svt* length that are greater than case of $k = 338.6$. In the end, the three cases have many data points that can be reached by the simulation curve or they have the large enough values of *ptp*.

5 Discussion

Based on the results of the research [25], it stated that the getting sharper surface shape of the electrode will produce a larger and sharper plasma discharge. Because the *S-ELTP* electrode configuration has a less sharp electrode shape, it is quite difficult to produce a sufficiently large and sharp plasma discharge at the lower end of the active electrode, so that the value of k produced in this experiment is not too large (only worth hundreds, not thousands).

From Table 1, it can be seen that the value of k is greater when the electrode size is larger. This fact is quite natural because a large electrode requires a larger voltage to produce a large plasma flow, as shown in Figures 5c and 5d. In the case of large electrodes size, the calculation from the *t-test* and *SD* turned out to produce quite large values, but still meets the boundary conditions for high accuracy values.

According to [26], the formulation of the (I–V) characteristic model in equation (2) will be more suitable if used at a short- distance of c. Producing the plasma discharge from a small electrode size model is quite difficult to do in this research because the *S-ELTP* electrode configuration has a less sharp shape at the lower end of the active electrode. We obtained research data at two different distances, namely at $c = 0.009$ m (short-distance) and $c = 0.033$ m (long-distance). In the case of c = 0.009 m, the value of $k = 338.6$ is obtained, which is smaller than the value of k in the case at distance $c = 0.033$ m. In the case of $c = 0.033$ m, it shows that there is a slight incompatibility with the concept of a fairly small distance between the two electrodes [26], resulting in a large enough value of $k = 547.8$, with a value of the *t-test* and *SD* scores which, although quite large, still meet the requirements of high accuracy.

From Figure 5, it can be seen that the shape of the simulation curve, which is calculated using equation (18), has various deviations from the position of the research data especially when approaching peak current conditions. However, the formulation in equation (18) is still quite suitable for the case of low currents before reaching the intermediate and peak currents, as clearly seen in Figure 5d for the value of $k = 547.8$. The match condition between numerical calculations and experimental data that only occurs in the case of low currents from corona plasma discharges is also found by [29].

This research does not discuss the physical phenomena that underlie the emergence of the corona currents, but only examines the visual phenomena of the corona currents that occur on the sharp surface of the active electrode. We realize that this research is not very perfect study, because in the most accurate case of the (I–V) characteristic graph ($k = 338.6$) it turns out to have small ntp and ptp values. However, if you look at the error values condition of the *t-test* and the *SD* measurements in general, all the (I–V) graphs have a high level of accuracy.

In this study, there are several shortcomings that greatly affect the quality of the research data that has been obtained, such as the level of accuracy quality that is less than the plasma reactor measurement equipment, less smooth electrode equipment, less careful observations of the researchers. Also, there is a factor of energy loss that occurs in plasma reactor equipment.

6 Conclusion

Although there are various shortcomings of the plasma reactor measurement equipment and the observations of researchers, we can conclude that the calculation of the current–voltage characteristics of the corona plasma discharge in the air from the *S-ELTP* configuration model has a high degree of compatibility between the calculation of the numerical curve and the research data points. There are three explanations that underlie this reason, namely: the first is based on the high research accuracy level obtained from the *t-test* value (lower than 0.05) and the small value of *SD* where the *Python GUI Programming* has created the (I–V) characteristic graph along with the calculation of the research accuracy. We get the highest accuracy of this research is obtained in the case of small electrodes size with a value of $c = 0.009$ m (the short-distance case). The second is that the calculation of the degree of compatibility between numerical calculations and research data is only suitable for the case of the low currents before reaching sharply increasing currents (the corona currents) as stated by [29]. Third, although this study is not a very perfect study, because it has the disadvantage of low *ntp* and *ptp* values for the most accurate research cases (at $k = 338.6$), in general, this research meets the accuracy high-level requirements, because it meets the standard requirements of the maximum values of the t-test and *SD* values for the *GUI* Programming.

The conclusion obtained from the results of this study is that the simulation calculation of the S-ELTP electrode configuration model is still quite feasible to be used as a reference for the formulation of corona discharge at low current conditions. In general, this research is quite simple because it uses a modified capacitance model. The model can be applied to other electrode models, as has been done by [12–14]. This research model is supported by the results of [25] experiment which visually can be seen that the sharper the active electrode, the greater the flow of corona current. Another impact of using the (I–V) characteristic calculation model is that we can determine dimensions and distance between the two electrodes of certain the CCP equipment in order to obtain the desired amount of corona current, which may be very useful for the industrial world.

The authors declare that they hold no competing interests.

This work was financially supported by non-tax revenue (PNBP), Diponegoro University, Semarang, Indonesia under contract No. 2196/UN7.5.8.2/PP/2021.

Author contribution statement

Asep Yoyo Wardaya: mathematical model, numerical calculation, and writing the part manuscript. Zaenul Muhlisin and Evi Setiawati: preparation of research equipment and experimental work. Jatmiko Endro Suseno and Susilo Hadi: simulation program and writing the part manuscript. Qidir Maulana Binu Soesanto and Muchamad Azam: discussion and writing the part manuscript. All authors have read and approved the final manuscript.

References

1. P.K. Shukla, A.A. Mamun, Introduction to Dusty Plasma Physics (CRC Press, Boca Raton Florida, 2001)
2. A.B. Stambouli, R. Benallal, N. Oudini, S.M. Mesli, R. Tadjine, Eur. Phys. J. Appl. Phys. **80**, 1 (2017)
3. P. Saikia, H. Bhuyan, M. Escalona, M. Favre, E. Wyndham, J. Maze, J. Schulze, Plasma Sources Sci. Technol. **27**, 1 (2018)
4. E.M. van Veldhuizen, W.R. Rutgers, in Corona Discharges: Fundamental and Diagnostics. *Frontiers in low temperature plasma diagnostics IV* (2001) pp. 40–49
5. Y. Zheng, B. Zhang, J. He, Phys. Plasmas. **22**, 023501 (2015)

6. Y. Guan, R.S. Vaddi, A. Aliseda, I. Novosselov, Phys. Plasmas. **25**, 083507 (2018)
7. E. Moreau, N. Benard, F. Alicalapa, A. Douyere, J. Electrostat. **76**, 194 (2015)
8. M. Robinson, IEEE Trans. Power Appl. Syst. **PAS-86**, 2 (1967)
9. M. Robinson, Transact. Am. Inst. Electr. Eng. Part I **80**, 143 (1961)
10. P. Giubbilini, J. Appl. Phys. **64**, 3730 (1988)
11. K. Yamada, J. Appl. Phys. **96**, 2472 (2004)
12. A.Y. Wardaya, Z. Muhlisin, A. Hudi, J.E. Suseno, M. Nur, A.W. Kinandana, J. Windarta, Eur. Phys. J. Appl. Phys. **89**, 3080 (2020)
13. S. Hadi, A.Y. Wardaya, Z. Muhlisin, J.E. Suseno, P. Triadyaksa, A. Khumaeni, M. Nur, J. Phys. Its Appl. **3**, 2 (2021)
14. A.Y. Wardaya, Z. Muhlisin, J.E. Suseno, M. Nur, P. Triadyaksa, A. Khumaeni, E. Sarwoko, J. Windarta, S. Hadi, Gazi Univ. J. Sci. (to be published), https://dergipark.org.tr/en/pub/gujs/issue/54905/885345
15. H. Abe, M. Yoneda, N. Fujiwara, J. Appl. Phys. **47**, 1435 (2008)
16. R. Siphehia, A. Garfinkle, W.B. Jackson, T.M.S. Chang, Biomat., Art. Cells. Art. Org. **18**, 643 (1990)
17. A. Anders, Surf. Coat. Technol. **200**, 1893 (2005)
18. H. Schmidt, L. Sansonnens, A.A. Howling, Ch. Hollenstein, M. Elyaakoubiand, J. P. M. Schmitt, J. Appl. Phys. **95**, 4559 (2004)
19. N. Benard, E. Moreau, N. Zouzou, H. Rabat, J. Pons, D. Hong, A. Leroy-Chesneau, P. Peschke, C. Hollenstein, "Nanosecond Pulsed Plasma Actuators", ERCOFTAC Bulletin No. 94 March 2013
20. X. Meng, H. Zhang, J. Zhu, J. Phys. D: Appl. Phys. **41**, 065209 (2008)
21. K. Yanallah, F. Pontiga, Plasma Sources Sci. Technol. **21**, 045007 (2012)
22. S. Chen, J. Nobelen, S. Nijdam, Plasma Sources Sci. Technol. **26**, 095005 (2017)
23. S.I. Wais, D.D. Giliyana, Am. J. Mod. Phys. **2**, 46 (2013)
24. P. Giubbilini, J. Appl. Phys. **81**, 2101 (1997)
25. J. Dobranszky, A. Bernath, H. Marton, Int. J. Microstruc. Mater. Propert. **3**, 1 (2008)
26. G.F.L. Ferreira, O.N. Oliveira Jr, J.A. Giacometti, J. Appl. Phys. **59**, 3045 (1986)
27. M.R. Spiegel, Mathematical Handbook of Formulas and Tables (Schaum 's Outline Series, New York, 1968)
28. I.S. Gradshteyn, I.M. Ryzhik, Table of Integrals, Series, and Products. 7th edn. (Academic Press, USA, 2007)
29. J.S. Townsend, Phil. Mag. (London). **28**, 83 (1914)
30. S. Boslaugh, Statistics in a nutshell: A Desktop Quick Reference (O'Reilly Media, Inc, USA, 2012)
31. C.H. Goulden, Methods of statistical analysis (John Wiley & Sons, Inc., New York, 1939)

Cite this article as: Asep Yoyo Wardaya, Zaenul Muhlisin, Jatmiko Endro Suseno, Qidir Maulana Binu Soesanto, Muchamad Azam, Evi Setiawati, Susilo Hadi, The electrode model of corona plasma discharge theory for current–voltage characteristics case in air, Eur. Phys. J. Appl. Phys. **97**, 22 (2022)